Abrardi, L., Martín-López, S., Carrasco-Sanz, A., Corredera, P., Hernanz, M.L., González-Herráez, M. "Optimized all-fiber supercontinuum source at 1.3 μm generated in a stepwise dispersion-decreasing-fiber arrangement", 2007, Journal of Lightwave Technology, 25 (8), pp. 2098-2102

Optimized all-fiber supercontinuum source at 1.3 μm generated in a stepwise dispersion decreasing fiber arrangement

L. Abrardi[1], **S. Martin-Lopez**[1], **A. Carrasco-Sanz**[1], **P. Corredera**[1], **M. L. Hernanz**[1]
1. *Instituto de Fisica Aplicada, Consejo Superior de Investigaciones Cientificas (CSIC)*
C/ Serrano 144, 28006 Madrid, Spain
M. Gonzalez-Herraez[2]
2. *Departamento de Electronica, Universidad de Alcala. Edificio Politecnico, Campus Universitario*
28871 Alcala de Henares, Madrid, Spain

The generation of a continuous-wave-pumped supercontinuum source at 1.3 μm is described. The device makes use of a tunable Yb-doped fiber laser, a cascade of fiber Bragg-grating mirrors and a concatenation of standard silica fibers with stepwise decreasing dispersion. It is shown that the dispersion decreasing fiber set enhances the width of the generated supercontinuum since it favors the fission of the cw input into high-order solitons. The generated supercontinuum spans from 1280 to 1513 nm, shows an average output power of 1.34 W and exhibits $>$0 dBm/nm spectral density over 200 nm.

Keywords: nonlinear optics, supercontinuum, soliton self-frequency shift

I. INTRODUCTION

Supercontinuum (SC) generation in optical fibers from continuous-wave (cw) laser has been studied intensively in the last years, both experimentally [1]–[9] and theoretically [10]–[12]. These broadband, high power density and low-coherence light sources have been found to be extremely useful for optical coherence tomography (OCT) [13], [14]. The preferred wavelength range in this case lies in the region of 1300 nm, since in this spectral interval the live tissue exhibits relatively low absorption and hence more penetration (see, for instance [15]).

Continuous-wave supercontinuum generation in fibers results from the fission of the partially coherent input cw beam into a sequence of Raman-shifted solitons through the combined effects of modulation instability (MI) and Stimulated Raman Scattering (SRS). Cw-induced spectral broadening is initiated by modulation instability (MI) which breaks-up the cw radiation into a train of ultrashort pulses when propagating in the wavelength region of small anomalous dispersion of the fiber. As the power is increased, the MI-generated pulses evolve into higher-order solitons (N-soliton) which, in turn, split into fundamental first order solitons (one-soliton) [11], [16] and undergo spectral shift towards longer wavelengths due to Stimulated Raman Scattering (SRS). This process of Soliton Self Frequency Shift (SSFS) gives rise to a smooth and wide spectrum lying at wavelengths longer than the pump wavelength. Additionally, each fundamental soliton can, in the presence of higher-order dispersion, release excess energy in the form of blueshifted dispersive waves, enhancing the spectral broadening on the shorter wavelength part of the supercontinuum. The mechanism of SC generation in this case is similar to SCs achieved using low-energy long pulses ($\sim$ps) in small anomalous dispersion regimes [16], [17].

The process of cw-pumped SC generation described above implies two restrictions from the point of view of the pump and the fiber used. First, the need of having an efficient MI implies that the pumping has to be done in the anomalous dispersion regime of the fiber. Second, since the cw-pumped SC spectra are typically composed of Raman-shifted solitons, the energy of the pump is mostly transferred to wavelengths that are longer than the pump wavelength. Thus, for the application of OCT, which requires having most of the SC energy around 1300 nm, most of the supercontinua developed up to now have been performed over photonic crystal fibers, which typically exhibit anomalous dispersion from below 1000 nm [18]. However, for compatibility with existing components, the development of SC sources based on conventional (all-silica) fibers results extremely interesting. With regards to this, most of the cw-pumped SC sources demonstrated up to now in conventional fibers have been developed using dispersion-shifted fibers [3], [7] and their spectrum lies typically at wavelengths longer than 1500 nm.

In this paper we present a new all-fiber design of cw-pumped SC source in the spectral range between 1.2 and 1.5 μm. The SC presented here relies on standard single-mode fibers, which have their zero-dispersion wavelength around 1.3 μm. The generated SC features an output power of 1.34 W and $>$0 dBm/nm spectral density over 200 nm. The spectral broadening is achieved by pumping in the small anomalous dispersion region of the fibers, which are arranged in stepwise decreasing dispersion order. In fact, according to recent theoretical results, dispersion decreasing fiber profiles can significantly improve the spectral broadening giving rise to shorter one-soliton pulse widths (hence broader spectra) [19].

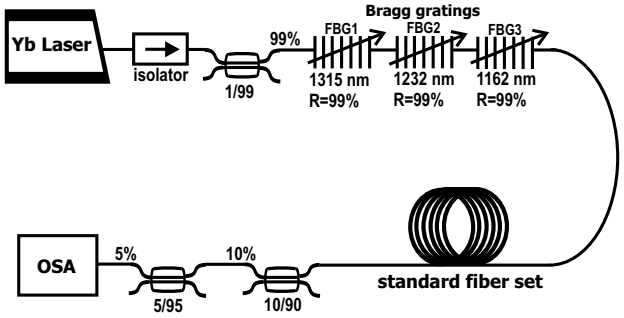

Fig. 1. Experimental setup. Yb laser: tunable Ytterbium-doped fiber laser emitting at 1104 nm; FBG: Fiber Bragg Gratings; OSA: Optical Spectrum Analyzer. The standard fiber set is made up of 4 fibers whose details can be seen in table I

	λ_0 nm	S_0 $ps/nm^2/km$	α (@ 1310 nm) dB/km	L km	D (@ 1315 nm) $ps/nm/km$
Fiber 1	1302	0.085	0.35	6.0	1.02
Fiber 2	1307	0.087	0.33	8.0	0.60
Fiber 3	1311	0.083	0.34	2.0	0.33
Fiber 4	1312	0.085	0.34	2.0	0.23

TABLE I

PROPERTIES OF THE SET OF OPTICAL FIBERS USED IN THE EXPERIMENT

This paper is organized as follows: in the following section the experimental setup is described; in Section III the SC source obtained from this experiment is reported; in section IV we discuss the importance of dispersion management on SC generation induced by MI in small anomalous dispersion regimes. Experimental results at low pump powers confirm that a dispersion decreasing fiber arrangement results in enhanced soliton fission. This is also in agreement with the results that we obtain in SC generation, where we empirically observed improved results for the dispersion decreasing fiber arrangement. Finally, we derive the conclusions of our study.

II. EXPERIMENTAL SET-UP

The experimental set-up is depicted in Fig.1. As a pump, we use a **commercial cw Yb-doped fiber laser (Keopsys KPS-BT2-TYFL-1100-200-FA) tuned at 1104 nm.** The output of the laser is single-mode with **line width >2 GHz, and tunable from 1080 nm to 1110 nm**. The power can take values from 0.57 to 20 W. **A pigtailed isolator (IO-K-1090 provided by OFR) at 1090 nm with and isolation spectral band of ∼30 nm around 1090 nm is inserted at the laser output to prevent damage in the laser by back-reflected light and backward Raman**. The isolator losses are approximately 2 dB. A 1/99 optical coupler is then introduced to monitor the power inserted into the fiber arrangement and the back-reflected power. To obtain efficient spectral broadening from cw laser in conventional fibers one needs to have the pump tuned at wavelengths in which the fiber exhibits small anomalous dispersion. Standard optical fibers have zero-dispersion wavelength (λ_0) around 1310 nm. Thus, to enable SC emission, we need to shift most of the laser power from 1100 nm to >1310 nm (where standard fibers exhibit small anomalous dispersion) to efficiently induce modulation instability (MI). In order to do this, we insert a cascade of Fiber Bragg Grating mirrors (FBGs) between the pump and the fiber set. As we will show in the next section, this arrangement allows to shift the laser emission at the desired wavelength without the need of a cavity. The FBGs have reflectivity >99% in all cases and total loss of 0.8 dB. Their bandwidths are centered at 1162 nm, 1232 nm and 1315 nm and have reflection bandwidths of 1.47 nm, 1.73 nm and 8.00 nm, respectively. FBG at 1315 nm has its maximum and minimum reflection at 1312 nm and 1320 respectively. The non-linear medium is made of a set of four standard single-mode fibers (SMF) of different λ_0 and lengths. The fibers are arranged in increasing λ_0 order (hence decreasing dispersion order). The choice of fiber lengths is dictated by the material available in our laboratory. The main properties of the fibers are reported in table I. The total fiber length is 18 km, which is one order of magnitude longer than typical lengths of the highly nonlinear fibers (HNLFs) used for cw-generated supercontinua. This agrees with the fact that conventional single-mode fibers exhibit a nonlinear coefficient which is one order of magnitude smaller than HNLFs. The output spectrum of our source is analyzed by means of an optical spectrum analyzer (OSA) after passing through two couplers, which act uniquely as fixed attenuators. The input and output power is measured by means of an integrating sphere radiometer whose responsivity at 1100 nm is 6 x 10^{-4} A/W with 1% uncertainty [20].

III. SUPERCONTINUUM GENERATION

The center wavelength of our laser is tuned at 1104 nm and hence it lies well within the normal dispersion regime of standard fibers. Therefore our first aim is to shift the wavelength of the laser to the spectral region of anomalous dispersion of the fibers by using a frequency-selective reflecting structure made of FBG mirrors. The process of wavelength shifting can be qualitatively described as follows: when we increase the laser pump power and we pass the Raman threshold we observe strong stimulated Raman scattering (SRS). Backward SRS appearing at 1162 nm is reflected back into the fiber by FBG3, and is subsequently amplified as it propagates in the forward direction. The emission at 1162 nm acts as a laser and plays a similar role to the pump laser. The same principle with FBG2 and FBG1 gives rise to cascaded Raman frequency generation ending up with a peak at 1315 nm which falls in the spectral region of small anomalous dispersion of the standard fibers used in the experiment.

In Fig.2 we can see the output spectrum for different pump powers (the values of pump power are measured at the input of the fibre set). When the input power takes the value of 1.16 W the first Raman peak at 1162 nm is clearly visible and the next Stokes order starts to appear (Fig.2(a)). At 2.37 W the second Raman peak at 1232 nm is also present. At this stage, depletion of the spectral lines at 1104 nm and 1162 nm also begins to occur. At input power level of 4.15 W the spectral lines at

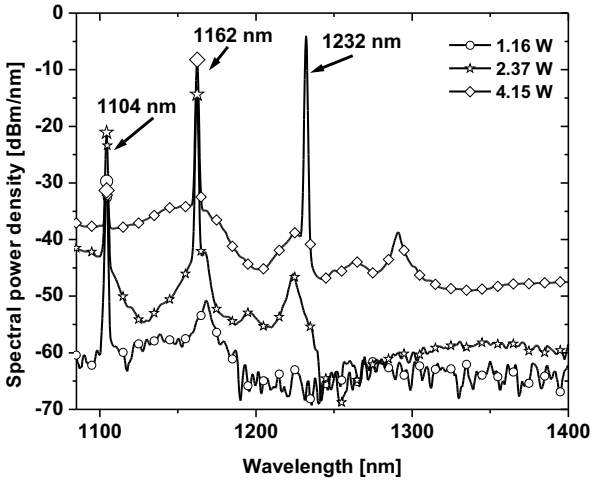

(a)

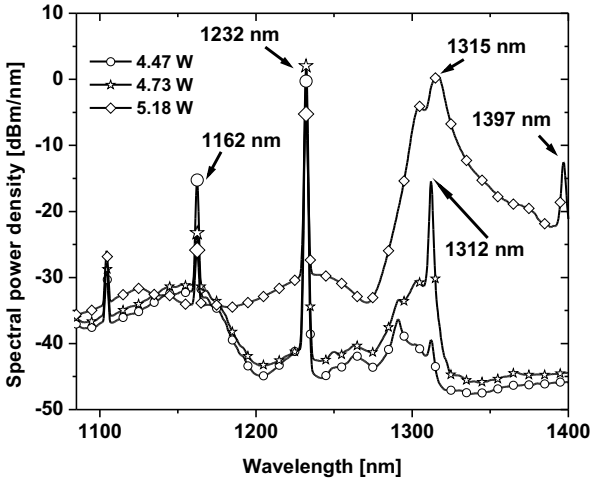

(b)

Fig. 2. Output spectra showing the Raman peaks at the output of the fibre set for different input powers. (a) Spectra for input powers of 1.16, 2.37 and 4.15 W. (b) Spectra for input powers of 4.47, 4.73 and 5.18 W; we can observe the evolution of the pump broadening around 1315 nm.

1104 nm and 1162 nm undergo almost full depletion and a peak at 1312 nm is clearly visible (Fig.2(b)). When the input power amounts to 4.73 W the spectral broadening starts to take place around 1315 nm. Earlier results have been reported on similar methods for the generation of cw SC emission [1], [2], [7], [21] which make use of a linear cavity configuration to shift the pump frequency into the anomalous dispersion region of the non-linear medium. It is worth to notice that, according to our results, a linear cavity is not strictly necessary to generate the spectral emission which will seed the SC broadening. As we can observe in Fig.2(b), at power levels higher than 4.5 W the spectral broadening around 1315 nm starts to take place and **another peak appears at 1397 nm. We are inclined to believe that this latter peak may be related to stimulated Raman scattering. This peak could also be potentialy attributed to FWM between the line at 1312 nm and the line at 1232 nm. However the frequency separation between the peak at 1397 nm and the peak at 1312 nm is estimated to be 13.9 THz and the frequency difference between the peak at 1312 nm and the peak at 1232 nm is 14.8 THz, hence not precisely the same, which should be the case if the process were induced by FWM. Besides that, it must be pointed out that the peak at 1312 nm broadens rapidly, and in comparison the peak at 1397 nm keeps much narrower at all power levels. In case it was FWM, the peak at 1397 nm should also broaden with power. Thus, we belive that the most probable origin of this peak is SRS, since the frequency separation is consistent with the Raman shift found in conventional fibers.** MI-induced soliton generation and Raman shift is also evident from the appearance of a smooth red-shifted tail in the pump spectrum.

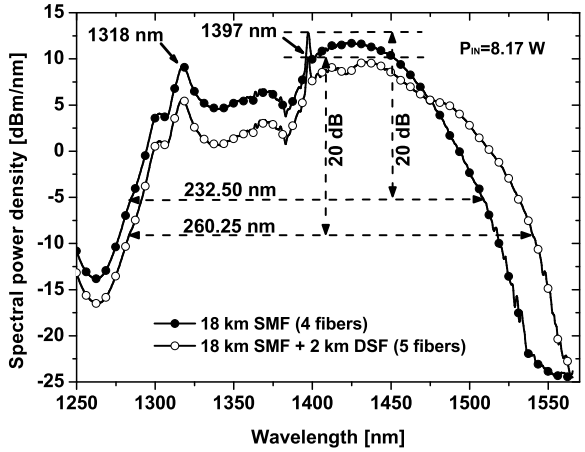

Fig. 3. Supercontinuum spectra for two different fiber configurations

In Fig.3 we show the SC spectrum obtained for two different fiber configurations. The first one (black circles) makes use of the set of fibers shown in table I arranged in dispersion-decreasing order. The input power is 8.17 W, while the SC output power is 1.36 W. The output spectrum spans over 232.5 nm as measured at 20dB from the highest peak and exhibits >0 dBm/nm spectral density over 200 nm. The Raman-induced asymmetric broadening towards longer wavelengths is clearly visible. A significant feature is the appearance of the peak at 1397 nm and a strong power transfer to the region between 1400 and 1450 nm, which is caused by forward SRS. **The conversion efficiency from the input pump at 1100 nm to the output SC is 16.6% at maximum input power.** To our knowledge, this is the broadest cw-pumped SC spectrum obtained by the only use of standard optical fibers.

The laser linewidth is such that stimulated Brillouin scattering is negligible, and in fact we have not measured any Brillouin backreflection in our setup. Backward Ra-

man scattering is also negligible in comparison with the total SC power in our experimental conditions (the power backreflected by Raman was less than 1% of the total SC power), hence there is no detrimental effect of this effect on the experiment at these power levels. Higher power levels, however, may result in a bigger impact of these effects.

To verify the role of dispersion management, we made the same experiment with the same set of fibers arranged in a different order. Since all the standard fibers used had essentially the same losses and the splice losses could be considered virtually negligible, we attribute any difference in the results solely to the dispersion profile used. None of the other arrangements that we tested (increasing dispersion, random dispersion) gave such an optimized spectrum as the dispersion decreasing fiber arrangement. The next section will aim at giving some experimental insight on why this dispersion arrangement yields the optimum results. This possibility, however, had also been theoretically proposed in recent works [19].

In a further demonstration of the possibilities offered by dispersion management, a dispersion-shifted fiber (DSF) is added at the end of the optimum fiber arrangement found above. The DSF is added at the end of the arrangement, in such a way as to keep a decreasing-dispersion configuration. This fiber is 2 km long and has its λ_0 at 1417 nm. Since a significant part of the SC power generated with the setup described above lies at wavelengths slightly above the λ_0 of this fiber, we expected that the insertion of this fiber would stimulate soliton fission in this spectral region and provide further spectral broadening. As it can be seen, this arrangement improves the spectral width of our SC. In this case (achieved for 8.17 W of input pump power) the SC spectrum spans $>$260 nm as measured at 20 dB from the highest peak, it has an output power of 0.840 W and exhibits > 0 dBm/nm spectral density over 214 nm.

IV. DISPERSION MANAGEMENT

In order to gain some insight on the role of dispersion management on the spectral broadening process, we perform an experiment at relatively low input power. In this way, we avoid the effect of SSFS and we can investigate the effect of dispersion management on the very first initial steps of soliton formation, which is driven mostly by MI. Spectral broadening is induced in two different fiber configurations: in the first one, the fibers are arranged in decreasing dispersion order, while in the second one the same fibers are arranged in increasing dispersion order, so as to operate with the same total fiber length.

We use the setup shown above (Fig.1) but a 11-km dispersion shifted fiber (DSF) is inserted between the FBGs and the SMF set. It has its λ_0 at 1552 nm and it does not affect the spectral broadening because we operate in the normal dispersion region of this fiber. Despite its total losses (7.2 dB), we use it to enhance the power transfer to the spectral wavelength of 1315 nm by SRS. In this way, MI can start at lower input power. In Fig.4 the spectra at the input (solid line) and output (black and white circles) of the standard fiber set are shown. The input spectrum clearly shows that the DSF does not affect the spectral broadening. The power at the input of the SMF set is 808.6 mW. The power at the output of the SMF set has been measured to be 182.4 mW for both arrangements with an uncertainty of 1%. This results clearly shows the importance of the dispersion profile on SC generation. The decreasing dispersion configuration (black circles) gives rise to a spectrum which is 50% larger than the increasing one. The presence of a much stronger blueshifted component in the dispersion decreasing arrangement is a clear signature of more efficient soliton formation, since this blueshifted component can only be explained as dispersive waves generated by the solitons in the presence of higher-order dispersion.

According to theory [19], [22], the unstable MI frequencies are inversely proportional to the square root of the dispersion so that the instability occurs at higher frequencies when dispersion is decreasing. This phenomenon affects the power transferred to the generated N-solitons, which, in their turn, can give rise to shorter one-soliton pulse widths (hence a broader spectrum). These fundamental solitons can undergo frequency shift towards longer wavelengths and emit blueshifted dispersive waves.

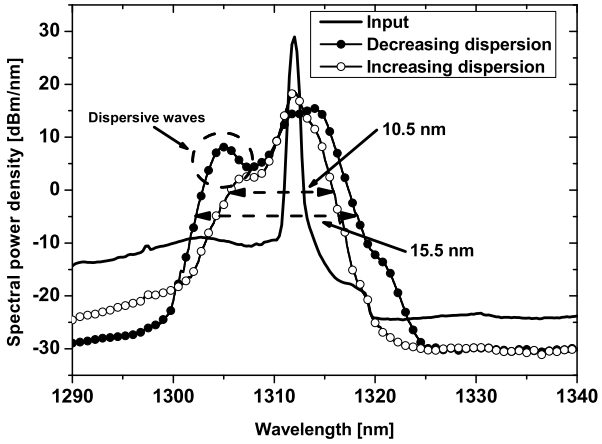

Fig. 4. Spectral broadening at the output of the fiber set. The spectral width is measured 20−dB down from the highest peak. The input spectrum is also reported (solid line).

V. CONCLUSIONS

We have demonstrated pump spectral broadening and supercontinuum generation spanning more than 232 nm in the spectral range of 1.2-1.5 μm. This has been achieved by pumping a concatenation of conventional fibers with an Yb-doped fiber laser and a frequency-selective reflective structure that seeds supercontinuum emission at 1315 nm, in the regime of small anomalous dispersion of the fibers used in the experiment. A stepwise dispersion fiber arrangement has been used which enhances the spectral broadening. We believe that such a SC profile is very promising for high power density, all-fiber

SC applications. This source seems particularly interesting for ultrahigh resolution OCT. Further investigation will be necessary to obtain a flatter spectral profile.

ACKNOWLEDGMENT

The authors would like to thank the financial support of Ministerio de Educacion y Ciencia through the project TIC2003-01869 and the corresponding FPI contract, the support from Comunidad Autonoma de Madrid through the projects FACTOTEM S-0505/ESP/0417 and FUTURSEN S-0505/AMB/000374 and the support of the Social European Fund through the I3P Grant Program of the CSIC.

REFERENCES

[1] M. Prabhu, N. S. Kim, and K. Ueda, "Ultra-broadband cw supercontinuum generation centered at 1483.4 nm from brillouin/raman fiber laser," *Japanese Journal of Applied Physics*, vol. 39, no. 4A, p. L291, 2000.

[2] M. Prabhu, A. Taniguhci, S. Hirose, J. Lu, M. Musha, A. Shirakawa, and K. Ueda, "Supercontinuum generation using raman fiber laser," *Applied Physics B*, vol. 77, no. 2-3, p. 205, 2003.

[3] M. Gonzalez-Herraez, S. Martin-Lopez, P. Corredera, M. L. Hernanz, and P. R. Horche, "Supercontinuum generation using a continuous-wave raman fiber laser," *Optics Communications*, vol. 226, no. 1-6, p. 323, 2003.

[4] J. W. Nicholson, A. K. Abeeluck, C. Headley, M. F. Yan, and C. G. Jorgensen, "Pulsed and continuous-wave supercontinuum generation in highly nonlinear, dispersion-shifted fibers," *Applied Physics B*, vol. 77, no. 2-3, p. 211, 2003.

[5] S. Martin-Lopez, M. Gonzalez-Herraez, P. Corredera, M. L. Hernanz, and A. Carrasco, "Gain flattening of fiber raman amplifiers using nonlinear pump spectral broadening," *Optics Communications*, vol. 242, no. 4-6, p. 463, 2004.

[6] P. A. Champert, V. Couderc, and A. Barthelemy, "1.5-2.0 μm multiwatt continuum generation in dispersion-shifted fiber by use of high-power continuous-wave fiber source," *Photonics Technology Letters*, vol. 16, no. 11, p. 2445, 2004.

[7] A. K. Abeeluck and C. Headley, "Supercontinuum growth in a highly nonlinear fiber with a low-coherence semiconductor laser diode," *Applied Physics Letters*, vol. 85, no. 21, p. 4863, 2004.

[8] A. K. Abeeluck, C. Headley, and C. G. Jorgensen, "High-power supercontinuum generation in highly nonlinear, dispersion-shifted fibers by use of a continuous-wave raman fiber laser," *Optics Letters*, vol. 29, no. 18, p. 2163, 2004.

[9] T. Sylvestre, A. Vedadi, H. Maillotte, F. Vanholsbeeck, and S. Coen, "Supercontinuum generation using continuous-wave multiwavelength pumping and dispersion management," *Optics Letters*, vol. 31, no. 13, p. 2036, 2006.

[10] A. Mussot, E. Lantz, H. Maillotte, T. Sylvestre, C. Finot, and S. Pitois, "Spectral broadening of a partially coherent cw laser beam in single-mode optical fibers," *Optics Express*, vol. 12, no. 13, p. 2838, 2004.

[11] F. Vanholsbeeck, S. Martin-Lopez, M. Gonzalez-Herraez, and S. Coen, "The role of pump incoherence in continuous-wave supercontinuum generation," *Optics Express*, vol. 13, no. 17, p. 6615, 2005.

[12] S. M. Kobtsev and S. V. Smirnov, "Modelling of high-power supercontinuum generation in highly nonlinear dispersion shifted fibers at cw pump," *Optics Express*, vol. 13, no. 18, p. 6912, 2005.

[13] J. G. Fujimoto, "Optical coherence tomography for ultra high resolution in vivo imaging," *Nature Biotechnology*, vol. 21, no. 11, p. 1361, 2003.

[14] P. L. Hsiung, Y. Chen, T. H. Ko, J. G. Fujimoto, C. J. S. de Matos, S. V. Popov, J. R. Taylor, and V. P. Gapontsev, "Optical coherence tomography using a continuous-wave, high power, raman continuum light source," *Optics Express*, vol. 12, no. 22, p. 5287, 2004.

[15] T. R. Hillman and D. D. Sampson, "The effect of water dispersion and absorption on axial resolution in ultrahigh-resolution optical coherence tomography," *Optics Express*, vol. 13, no. 6, p. 1860, 2005.

[16] A. V. Husakou and J. Hermann, "Supercontinuum generation of higher-order solitons by fission in photonic crystal fibers," *Physical Review Letters*, vol. 87, no. 20, pp. 203 901–1, 2001.

[17] J. Hermann, U. Griebner, N. Zhavoronkov, A. Husakou, D. Nickel, J. C. Knight, W. J. Wadsworth, P. S. J. Russel, and G. Korn, "Experimental evidence for supercontinuum generation by fission of higher-order solitons in photonic fibers," *Physical Review Letters*, vol. 88, no. 17, p. 173901, 2002.

[18] J. C. Travers, S. V. Popov, and J. R. Taylor, "Extended cw supercontinuum generation in a low water-loss holey fiber," *Optics Letters*, vol. 30, no. 23, p. 3132, 2005.

[19] J. N. Kutz, C. Lynga, and B. J. Eggleton, "Enhanced supercontinuum generation through dispersion-management," *Optics Express*, vol. 13, no. 11, p. 3989, 2005.

[20] A. Carrasco-Sanz, F. Rodriguez-Barrios, P. Corredera, S. Martin-Lopez, M. Gonzalez-Herraez, and M. L. Hernanz, "An integrating sphere radiometer as a solution for high power calibrations in fibre otpics," *Metrologia*, vol. 43, no. 2, p. S145, 2006.

[21] M. Feng, Y. G. Li, J. Li, J. F. Li, L. Ding, and K. C. Lu, "High-power supercontinuum generation in a nested linear cavity involving a cw raman fiber laser," *Photonics Technology Letters*, vol. 17, no. 6, p. 1172, 2005.

[22] G. P. Agrawal, *Applications of Nonlinear Fiber Optics*. Academic Press, 2001.